Use of an advanced shear-lag model to obtain the optimum internal damping in short-fiber composites

P Hajela and C-J Shih

Aerospace Engineering, Mechanics and Engineering Science, University of Florida, Gainesville FL 32611

The present paper examines a modified shear-lag model for predicting the stress distribution in short fiber reinforced composite materials. The model assumes perfect bonding between the fiber and the matrix materials, and allows for the matrix material to partially sustain axial loads. The stress distribution obtained on the basis of this model is used to predict the internal damping characteristics of the composite material. These characteristics are a function of both the material properties and the geometrical layout of the composite, and are optimized by combining the analytical model with a nonlinear programming optimization algorithm. Representative numerical results are obtained for glass–epoxy and graphite–epoxy composites.

1. INTRODUCTION

Internal material damping in composites depends on the properties of the fiber and matrix materials, and on the geometrical layout of the composite. Glass and graphite reinforced polymer matrix composites exhibit anisotropic, linear viscoelastic behavior. The principal mechanism of damping in such composites is considered to be the viscoelastic energy dissipation in the matrix material. Experimental investigations reported by McLean and Read (1975) and Gibson and Yau (1980) indicate that the damping in discontinuous fiber composites is in general greater than that in continuous fiber composites. This can be partly attributed to the stress concentration effects at fiber ends, which facilitates the dissipation of energy in the viscoelastic matrix material.

The first attempt to tailor the damping properties of composite structures can be traced to an effort due to Plunkett and Lee (1970). Several models have been proposed for predicting the damping in short fiber reinforced composites. Gibson et al (1982) discuss a formulation for obtaining the internal damping for a case in which the load is applied parallel to the fiber direction. The elastic–viscoelastic correspondence principle was used in conjunction with both an energy formulation and a force balance procedure to obtain the analytical predictions of damping. This approach is based on a shear-lag analysis of Cox (1952), which assumes that the stresses at the fiber ends vanish, and that the matrix material carries no axial load. Results obtained in the analysis are shown to be in good agreement with experimental data.

Sun et al (1985) have developed theoretical relationships for the material damping of short fiber-reinforced polymer matrix composites under off-axis loading. They develop relations for the loss and storage modulus in terms of fiber aspect ratio, loading angle, stiffness of the fiber and matrix materials, the volume fraction, and the damping properties of the fiber and matrix materials. They also conduct parametric studies to examine the variation of the damping with the fiber aspect ratio and the loading angle, to determine optimum values of these parameters for maximum internal damping. Parametric studies of the type described above in design synthesis procedures have been shown to yield suboptimal results. The present paper proposes a design synthesis approach based on formal multidimensional optimization that circumvents some of these problems.

In the present work, a force distribution approach similar to the one proposed by Fukuda and Chou (1981) is used to develop relations for the loss and storage modulii of the composite in terms of fiber aspect ratio, loading angle, stiffness of fiber and matrix materials, the fiber volume fraction, and the damping properties of the constituent materials. This advanced shear-lag model represents a departure from the Cox's model in that the matrix material is assumed to participate in the load carrying process. This analysis is then posed as a formal multivariable optimization problem to maximize the ex-

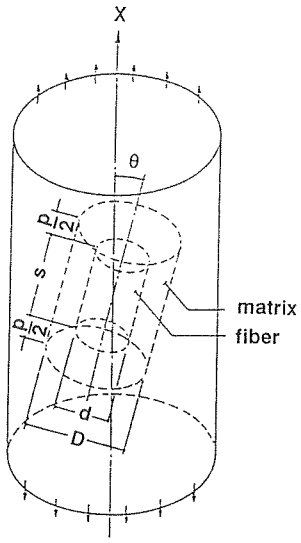

FIG. 1. Representative volume element for a short fiber composite.

tensional loss factor of a representative volume element shown in Fig. 1, with constraints on element mass and stiffness characteristics.

2. ADVANCED SHEAR-LAG MODEL

The composite structure is assumed to consist of a repeating sequence of short fibers, aligned unidirectionally and distributed uniformly in the structure. Hence, the model needed for developing the force distribution in the fibers and matrix is a two-dimensional arrangement of a three-fiber representative element shown in Fig. 2. The spacing between neighboring fibers is assumed to be constant and is indicated by h. An off-axis loading is assumed, with the fibers oriented at an angle θ with respect to the loading direction. The distance along the fiber direction is denoted by a nondimensional parameter $\xi = x/t$. As shown in Fig. 2, there are three distinct regions along this nondimensional coordinate denoted by $j = 1$, 2, and 3, where the force distribution is likely to change due to the presence, or lack thereof, of adjacent fibers. In this representative region, the fibers are numbered from $i = 1$ to $i = 3$, as shown in the figure.

As stated before, the model in the present work allows for the matrix to partially sustain axial loads. This is

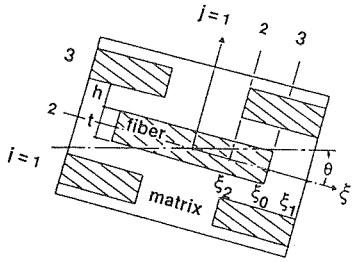

FIG. 2. A 2D three fiber model.

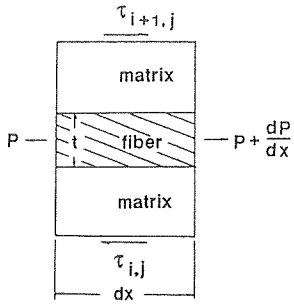

FIG. 3. Free-body diagram of middle fiber.

admitted by assuming the matrix material between two fiber ends, and of the same diameter as the fibers, behaves as a fiber with a different value of the Young's modulus, ie, the matrix material between the fibers is considered an extension of the fiber. The free body diagram of the middle fiber is shown in Fig. 3. The following differential equations are obtained from force equilibrium considerations in the x direction:

$$\frac{dP_{1j}}{dx} + \tau_{1j} = 0, \tag{1}$$

$$\frac{dP_{2j}}{dx} + \tau_{2j} - \tau_{1j} = 0, \tag{2}$$

$$\frac{dP_{3j}}{dx} - \tau_{2j} = 0. \tag{3}$$

Here P_{ij} and τ_{ij} are the axial force per unit thickness and interfacial shear stress in the ith fiber and jth region, respectively. The normal fiber stress and the interfacial shear can be written in terms of a displacement u_{ij} as follows:

$$\sigma_{ij} = E_{ij}\frac{du_{ij}}{dx}, \tag{4}$$

$$\tau_{ij} = G_m(u_{i+1} - u_{ij})/h, \tag{5}$$

where E_{ij} is the Young's modulus of region i–j, and the G_m is shear modulus of the matrix material; E_{ij} is either E_f (Young's modulus of the actual fiber) or E_m (Young's modulus of the matrix) depending upon the region j under consideration. Introducing a nondimensional parameter α_{ij} as

$$\alpha_{ij} = E_{ij}h/Gt \tag{6}$$

Eqs (1)–(3) can be rewritten as follows:

$$\alpha_{1j}u''_{1j} + u_{2j} - u_{1j} = 0, \tag{7}$$

$$\alpha_{2j}u''_{2j} + u_{3j} - 2u_{2j} + u_{1j} = 0, \tag{8}$$

$$\alpha_{3j}u''_{3j} - u_{3j} - u_{2j} = 0, \tag{9}$$

where

$$u''_{ij} = \frac{d^2u_{ij}}{d\xi^2}. \tag{10}$$

Equations (7)–(9) yield a solution of u_{ij} as a function of ξ, which can be used with Eq (5) to yield a set of

equations expressing P_{ij} as a function of ξ. Using conditions of symmetry and continuity of displacements and stresses at ξ_0, ξ_1, and ξ_2, a solution for the axial load variation in the composite P_{ij}, is obtained as a function of nondimensional spatial location $\xi = x/t$ and the ratio of the matrix and fiber tensile modulii $k = E_m/E_f$ as follows:

$$P_{21} = \frac{3P_0}{(1+2k)}\left[1 - \frac{8k\lambda_1 G(1-k)\cosh\lambda_1\xi}{3F}\right], \tag{11}$$

$$P_{22} = P_0\left[1 + \frac{2(1-k)}{(1+2k)}\cosh\lambda_2(\xi-\xi_2)\left(1-\frac{4GH}{F}\right)\right], \tag{12}$$

$$P_{32} = P_{12} = P_0\left[1 - \frac{(1-k)}{(1+2k)} \times \cosh\lambda_2(\xi-\xi_2)\left(1-\frac{4GH}{F}\right)\right], \tag{13}$$

$$P_{33} = P_{13} = \frac{3P_0}{(2+k)} \times \left[1 + \frac{\lambda_3 k(1-k)\cosh\lambda_3(\xi_1-\xi)}{\lambda_2(1+2k)\sinh\lambda_3(\xi_3-\xi_0)}\sinh\lambda(\xi_2-\xi_0)_2 \times\left(1-\frac{4GW}{F}\right)\right], \tag{14}$$

where

$$F = (2+k)\sinh\lambda_3(\xi_1-\xi_0) \times\left[4k\lambda_1\lambda_2\cosh\lambda_1\xi_2\cosh\lambda_2(\xi_0-\xi_2) + \frac{4(1+3k)\lambda_2^2}{3}\sinh\lambda_1\xi_2\sinh\lambda_2(\xi_0-\xi_2)\right] + \left[12k^2\lambda_1\lambda_3\cosh\lambda_1\xi_2\cdot\sinh\lambda_2(\xi_0-\xi_2) + 4k(1+3k)\lambda_2\lambda_3\sinh\lambda_1\xi_2\cosh\lambda_2(\xi_0-\xi_2)\right] \cdot\cosh\lambda_3(\xi_1-\xi_0), \tag{15}$$

$$G = \lambda_2\sinh\lambda_3(\xi_1-\xi_0) \times[1+2k+(2+k)\cosh\lambda_2(\xi_0-\xi_2)] + 3k\lambda_3\sinh\lambda_2(\xi_0-\xi_2)\cosh\lambda_3(\xi_1-\xi_0), \tag{16}$$

$$H = \frac{\lambda_2(1+3k)}{3}\sinh\lambda_1\xi_2\tanh\lambda_2(\xi_0-\xi_2) + \lambda_1 k\cosh\lambda_1\xi_2, \tag{17}$$

$$W = \frac{\lambda_2(1+3k)}{3}\sinh\lambda_1\xi_2\coth\lambda_2(\xi_0-\xi_2) + \lambda_1 k\cosh\lambda_1\xi_2, \tag{18}$$

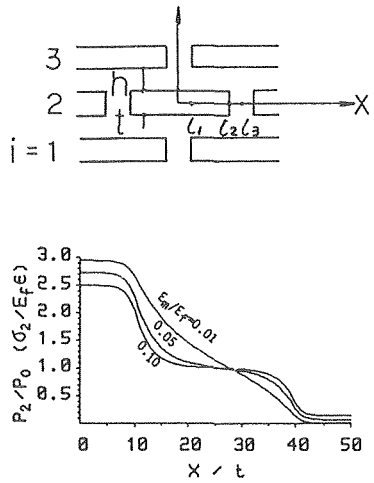

FIG. 4. Load distribution along middle fiber and matrix.

and λ_j is expressed as

$$\lambda_j = \left(\frac{\alpha_{2j}+2\alpha_{3j}}{\alpha_{2j}\alpha_{3j}}\right)^{0.5}. \tag{19}$$

The load distribution (or stress distribution) in the middle short fiber and in the matrix material between the fibers for the three fiber model, and for selected values of $k = E_m/E_f$ is shown in Fig. 4. These plots were obtained by assuming values of $h/t = 1$, $l_1/t = 10$, $l_2/t = 40$, $l_3/t = 50$, and $G_m/E_m = 14/34$. For k close to zero, one observes the expected zero loads at the fiber end. A similar trend in the outer fiber and matrix is observed, as shown in Fig. 5.

The average axial force $\bar{P}_{ij}$ can be obtained by integrating the force expressions $P_{ij}(\xi,k)$ over the fiber

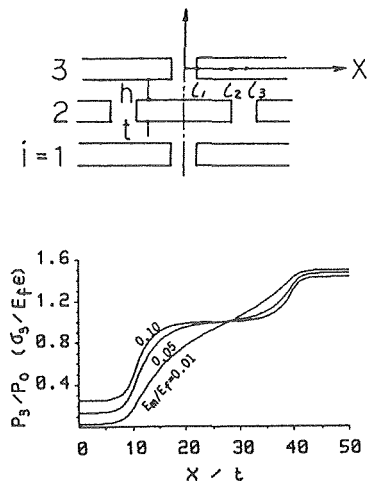

FIG. 5. Load distribution along outer fiber and matrix.

length:

$$\bar{P}_{21} = \frac{3P_0}{1+2k}\left[1 - \frac{16G}{3F}\frac{k\lambda_1(1-k)\sinh(\Sigma p/2)}{\Sigma p}\right], \quad (20)$$

$$\bar{P}_{22} = P_0\left[1 + \frac{4(1-k)}{\Gamma(s-p)(1+2k)} \times \sinh\frac{\Gamma}{2}(s-p)\left(1 - \frac{4GY}{F}\right)\right], \quad (21)$$

$$\bar{P}_{32} = \bar{P}_{12} = P_0\left[1 - E\frac{2(1-k)}{\Gamma(s-p)(1+2k)} \times \sinh\frac{\Gamma}{2}(s-p)\left(1 - \frac{4GY}{F}\right)\right], \quad (22)$$

$$\bar{P}_{33} = \bar{P}_{13} = \frac{3P_0}{(2+k)}\left\{1 + \frac{2\lambda_3 k(1-k)}{\Lambda p\lambda_2(1+2k)} \times \left[\sinh\frac{\Gamma}{2}(s-p) - \frac{4GW}{F}\right]\right\}, \quad (23)$$

where

$$Y = \frac{\lambda_2(1+3k)\sinh\frac{\Sigma}{2}p\left[\cosh\frac{\Gamma}{2}(s-p) - 1\right]}{3\sinh\frac{\Gamma}{2}(s-p)} + \lambda_1 k\cosh\frac{\Sigma}{2}p, \quad (24)$$

$$\Sigma = \frac{\lambda_1}{d} = \frac{1}{d}\left[\frac{G_m(E_f + 2E_m)}{E_f E_m\sqrt{(\pi/4V_f)(1+p/s)} - 1}\right]^{0.5}, \quad (25)$$

$$\Gamma = \frac{\lambda_2}{d} = \frac{1}{d}\left[\frac{3G_m}{E_f\sqrt{(\pi/4V_f)(1+p/s)} - 1}\right]^{0.5}, \quad (26)$$

$$\Lambda = \frac{\lambda_3}{d} = \frac{1}{d}\left[\frac{G_m(E_m + 2E_f)}{E_m E_f\sqrt{(\pi/4V_f)(1+p/s)} - 1}\right]^{0.5}. \quad (27)$$

Substitution of $\bar{P}_{ij} = A_f\bar{\sigma}_{ij}$ and $P_0 = A_f\epsilon E_f$ allows one to obtain expressions for the average stress in each region of the fiber, denoted as $\bar{\sigma}_{21}$, $\bar{\sigma}_{22}$, $\bar{\sigma}_{32}$, and $\bar{\sigma}_{33}$. The average stress in a representative fiber length s can be obtained by an expression based on geometrical considerations as follows:

$$\sigma_a = (1/3s)\{\bar{\sigma}_{21}p + \bar{\sigma}_{22}(s-p) + 2[\bar{\sigma}_{32}(s-p) + \bar{\sigma}_{33}p]\}. \quad (28)$$

For static equilibrium under the applied load, an expression for the stress in the composite specimen σ_c can be written by invoking a modified rule of mixtures.

$$\sigma_c = \sigma_a V_f(1+p/s) + \sigma_m[1 - V_f(1+p/s)], \quad (29)$$

where V_f is the fiber volume fraction of representative volume element. Substituting the value for the average fiber stress from Eq (28), and the matrix stress σ_m by $E_m G_m$ into Eq (29), and assuming equal axial strain in fiber and matrix materials, one can write an expression for the longitudinal modulus of representative volume element of composite between the section of fiber length E_c as follows:

$$E_c = E_f V_f(1+p/s)[1 - 2\tanh(\beta s/2)/\beta s] + E_m[1 - V_f(1+p/s)]. \quad (30)$$

When the same external stress σ is applied to short fiber composite model and to its equivalent homogeneous material model, equivalent strain energies may be assumed for these two models. Based on this assumption, the longitudinal Young's modulus E_L of the short fiber composite model can be expressed as follows:

$$E_L = \frac{E_c E_m}{E_c\frac{p/s}{1+p/s} + E_m\frac{1}{1+p/s}}. \quad (31)$$

In the present analysis, both fiber and matrix materials were assumed to be viscoelastic. The elastic–viscoelastic correspondence principle can be used to define the extensional and shear modulii as the following complex quantities:

$$E_x^* = E_x' + iE_x'', \quad (32)$$

$$E_f^* = E_f' + iE_f'', \quad (33)$$

$$E_m^* = E_m' + iE_m'', \quad (34)$$

$$G_m^* = G_m' + iG_m''. \quad (35)$$

Subscripts f and m denote fiber and matrix materials, and the prime and double prime quantities represent the storage and loss modulii, respectively. The ratio E_x''/E_x' is the loss factor and is a measure of the internal damping. With these definitions, the complex representation of Eq (31) is written as follows:

$$E_L^* = E_c^* E_m^*\left(E_c^*\frac{p/s}{1+p/s} + E_m^*\frac{1}{1+p/s}\right)^{-1}, \quad (36)$$

where

$$E_c^* = E_f^* V_f(1+p/s)[1 - 2\tanh(\beta^* s/2)/\beta^* s] + E_m^*[1 - V_f(1+p/s)]. \quad (37)$$

Here, the parameter $\beta^* s$ depends on the geometrical arrangement of the fibers in the matrix. For square packing geometry,

$$\beta^* s = 4\left(\frac{s}{d}\right)\left[\frac{G_m^*}{E_f^*\ln(\pi/4V_f)}\right]^{0.5}, \quad (38)$$

and for hexagonal packing geometry,

$$\beta^* s = 4\left(\frac{s}{d}\right)\left[\frac{G_m^*}{E_f^*\ln(\pi/2\sqrt{3}V_f)}\right]^{0.5}. \quad (39)$$

The Halpin–Tsai equations available in Agarwal and

Broutman (1980), in conjunction with the rule of mixtures, allows one to write expressions for the transverse modulus E_T^* and the in-plane shear modulus G_{LT}^*:

$$E_T^* = E_m^* \left(\frac{1 + 2\eta_1 V_f}{1 - \eta_1 V_f} \right), \tag{40}$$

$$G_{LT}^* = G_m^* \left(\frac{1 + \eta_2 V_f}{1 - \eta_2 V_f} \right), \tag{41}$$

where η_1 and η_2 are defined as follows:

$$\eta_1 = (E_f^*/E_m^* - 1)/(E_f^*/E_m^* + 2), \tag{42}$$

$$\eta_2 = (G_f^*/G_m^* - 1)/(G_f^*/G_m^* + 1). \tag{43}$$

Further, the Poisson ratio can be expressed as

$$\nu_{LT} = V_f \nu_f (1 + p/s) + \nu_m [1 - V_f (1 + p/s)]. \tag{44}$$

Here, ν_f and ν_m are the Poisson ratio for the fiber and matrix materials, respectively. With the above definitions, the modulus E_x^* assumes the following form:

$$\frac{1}{E_x^*} = \frac{1}{E_x' + iE_x''} = \frac{\cos^4\theta}{E_L^*} + \frac{\sin^4\theta}{E_T^*} + \left(\frac{1}{G_{LT}^*} - \frac{2\nu_{LT}}{E_L^*} \right) \sin^2\theta \cos^2\theta. \tag{45}$$

Equation (45) can be separated into real and imaginary parts to yield values of the storage and loss modulii. As defined before, the loss factor is then expressed as follows:

$$\eta_x = E_x''/E_x'. \tag{46}$$

The shear loss factor is defined as the ratio of the storage to loss components of the shear modulus, where the latter are obtained from the expression shown below

$$\frac{1}{G_{xy}^*} = \frac{1}{G_{xy}' + iG_{xy}''} = \frac{1}{E_L^*} + \frac{2\nu_{LT}}{E_T^*} + \frac{1}{E_T^*} - \left(\frac{1}{E_L^*} + \frac{2\nu_{LT}}{E_L^*} + \frac{1}{E_T^*} - \frac{1}{G_{LT}^*} \right) \cos^2 2\theta. \tag{47}$$

3. OPTIMUM SYNTHESIS PROBLEM

To study the optimum layout of the composite specimen for maximum internal damping, the problem was posed as a nonlinear optimization problem with an objective to maximize η_x, which is a function of the design variable vector $V = \{E_f^*, E_m^*, G_m^*, p, s, d, D, \theta\}$, and subject to upper and lower bound constraints on the mass and extensional stiffness of the composite specimen. The inequality and side constraints in the present problem were formulated for nominal values of lower and upper bounds on the geometric variables and are as follows:

$$\sigma_{fu}/2\tau_y \le s/d \le 1000, \tag{48}$$

$$d \le D - 0.001, \tag{49}$$

$$0.01 \le p/s, \tag{50}$$

$$0 \le \theta \le \pi/2, \tag{51}$$

$$0.5 \le V_f \le \pi/4 \quad \text{(square packing)}, \tag{52}$$

$$0.5 \le V_f \le \pi/2\sqrt{3} \quad \text{(hexagonal packing)}. \tag{53}$$

Here σ_{fu} is the ultimate strength of short fiber, and τ_y is the matrix yield stress in shear. The constraint of Eq (48) stems from considerations of the critical fiber length, as developed in Agarwal and Broutman (1980). In this study, the σ_{fu} of glass fiber and graphite fiber were selected as 3500 and 2750 Mpa, respectively, and a matrix yield shear stress value of 97 Mpa was adopted. The volume fraction V_f can be expressed for square and hexagonal packing arrangement as follows:

$$V_f = \pi d^2/[4D^2(1 + p/s)] \quad \text{(square)}, \tag{54}$$

$$V_f = \pi d^2/[2\sqrt{3}\, D^2(1 + p/s)] \quad \text{(hexagonal)}. \tag{55}$$

The mass of a representative volume element can be written as

$$m = (\pi/4)\{\rho_f s d^2 + \rho_m [pD^2 + s(D^2 - d^2)]\}, \tag{56}$$

where ρ_f and ρ_m denote the specific weight of the fiber and matrix materials, respectively. In addition to constraints given by Eqs (48)–(53), additional inequality constraints can also be imposed on the mass of the representative volume element and the extensional stiffness of the composite specimen. The latter constraint allows for tailoring the damping requirement of the specimen, with added specification on its load-deflection characteristics.

The optimization problem described above can be solved by any of the known methods of nonlinear programming. Zoutendijk's method of feasible-usable search directions, as presented in Vanderplaats (1984) was used as the optimization algorithm in the present problem to generate a sequence of optimum designs.

4. RESULTS AND DISCUSSIONS

An optimum design approach such as the one used here allows for a systematic study of composite layout

TABLE I. MATERIAL PROPERTIES OF THE MATRIX AND FIBER MATERIALS

Constants	Matrix	Fibers	
	Epoxy	Glass	Graphite
E_L (Gpa)	3.4	72.4	228.
E_T (Gpa)	3.4	72.4	13.8
G_{LT} (Gpa)	1.4	$E_L/[2(1+\nu)]$	27.6
ν_{LT}	0.4	0.2	0.16
η	0.015	0.0014	0.0014
η_G	0.018	—	—
$\rho(kg/m^3)$	1220	2539	1760

TABLE II. OPTIMUM DESIGN FOR GLASS–EPOXY COMPOSITE USING MODIFIED SHEAR-LAG ANALYSIS, $(\Sigma F_U/2T_Y - \leq S/D$ (LENGTH UNITS IN MM)

Packing	k	d	D	P	s	θ	V_f	s/d	η_x
Square	0.	0.01	0.0124	0.039	0.197	49.5	0.5	19.7	0.01489
	0.047	0.01	0.0124	0.029	0.189	50.8	0.5	18.9	0.01487
Hexagonal	0.	0.01	0.0134	0.029	0.20	49.7	0.5	20.0	0.01489
	0.047	0.01	0.0134	0.029	0.196	50.4	0.5	19.6	0.01487

TABLE III. OPTIMUM DESIGN FOR GLASS–EPOXY COMPOSITE WITH CONSTRAINT ON EXTENSIONAL MODULUS OBTAINED BY USING MODIFIED SHEAR-LAG ANALYSIS, $(\Sigma F_U/2T_Y) \leq S/D$ (LENGTH UNITS IN MM)

Packing	k	d	D	P	s	θ	V_f	s/d	η_x
Square	0.	0.01	0.0119	0.040	0.227	45.8	0.55	22.7	0.01455
	0.047	0.01	0.0119	0.034	0.188	51.0	0.56	18.5	0.01445
Hexagonal	0.	0.01	0.0128	0.030	0.197	45.9	0.55	19.7	0.01455
	0.047	0.01	0.0127	0.040	0.180	47.2	0.55	18.0	0.01450

TABLE IV. OPTIMUM DESIGN FOR GRAPHITE—EPOXY COMPOSITE WITH CONSTRAINT ON EXTENSIONAL MODULUS OBTAINED BY USING MODIFIED SHEAR-LAG ANALYSIS, $(\Sigma F_U/2T_Y) \leq S/D$ (LENGTH UNITS IN MM)

Packing	k	d	D	P	s	θ	V_f	s/d	η_x
Square	0.	0.0053	0.0054	0.037	0.096	18.0	0.55	18.0	0.01493
	0.015	0.0053	0.0054	0.034	0.098	19.7	0.56	18.4	0.01487
Hexagonal	0.	0.0053	0.0062	0.024	0.075	20.1	0.5	14.2	0.01458
	0.015	0.0053	0.0062	0.024	0.079	20.7	0.5	14.8	0.01457

without resorting to a parametric study, an approach that frequently yields suboptimal results. A range of optimal geometric configurations can be obtained for prescribed loadings, and for bounds on parameters such as mass and stiffness of the specimen. All material properties used in the numerical work are summarized in Table I. A typical optimum design with constraint on the element mass is illustrated in Table II. The final results for isotropic glass fiber composite, with a constraint on the extensional stiffness are summarized in Table III. Similar results for orthotropic graphite fiber composite are shown in Table IV.

The load distributions in the middle and outer fibers, as shown in Figs. 4 and 5, are in accordance with expected values. With reference to Fig. 4, a large axial load is carried by the fiber at $x/t = 0$. This load remains more or less constant till x/t increases to the point that the outer two fibers participate in the load carrying process. At this point, there is a drop-off in the load in the central fiber. When x/t increases further to the end of the central fiber, the load drops to a near zero value for a value of $k = 0.0$. This is in agreement with Cox's shear-lag analysis. For finite values of k, there is a finite axial load at the fiber end, albeit a small one. Similar arguments can be made about the load variations in the outer fiber shown in Fig. 5.

Variation in the optimum loss factor for prescribed extensional stiffness requirements is illustrated in Fig. 6. This figure depicts the dependence of the loss factor on k, with three specific values of k chosen for comparison. The case $k = 0$ illustrates the Cox shear-lag analysis for a

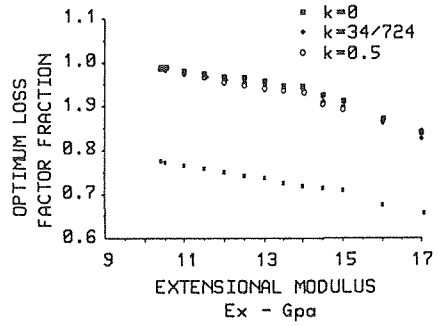

FIG. 6. Variation of loss factor with stiffness and $k = E_m/E_f$ (*: $k = 0.141$, $\eta_m = 0.012$, $\eta_{Gm} = 0.014$).

glass–epoxy composite and $k = 0.047$ and $k = 0.5$ correspond to an analysis based on the advanced shear-lag model for the same material. A hypothetical matrix material is represented as the fourth case, with $k = 0.141$ associated with $\eta_m = 0.012$ and $\eta_{Gm} = 0.014$. With increasing values of k, the optimum damping is lower. This is to be expected as the matrix contributes to the axial load carrying capability, generating lower interfacial shear, and hence a lower energy dissipation in the matrix material. The Cox model appears to be adequate for analysis of composites with polymer matrix materials, where the extensional modulus of the matrix material is low. However, alternate shear-lag models must be explored for matrix materials with higher extensional modulii, in particular, metal matrix composites.

REFERENCES

Agarwal, B D, and Broutman, L J (1980), *Analysis and performance of fiber composites*, 1st ed, Wiley, New York.

Cox, H L (1952), The elasticity and strength of paper and other fibrous materials, *Br J Appl Phys* **3**, 72–79.

Fukuda, H, and Chou, T W (1981), An advanced shear-lag model applicable to discontinuous fiber composites, *J Compos Mat* **15**, 79–91.

Gibson, R F, and Yau, A (1980), A complex modulii of chopped fiber and continuous fiber composites: comparison of measurement with estimated bounds, *J Compos Mat* **14**, 155–167.

Gibson, R F, Chaturvedi, S K, and Sun, C T (1982), Complex modulii of aligned discontinuous fiber-reinforced polymer composites, *J Mat Sci* **17**, 3499–3509.

McLean, D, and Read, B W (1975), Storage and loss modulii in discontinuous composites, *J Mat Sci* **10**, 481–492.

Plunkett, R, and Lee, C T (1970), Length optimization for constrained viscoelastic layer damping, *J Ac Soc Am* **48**, 150–161.

Sun, C T, Gibson, R F, and Chaturvedi, S K (1985), Internal material damping of polymer matrix composite under off-axis loading, *J Mat Sci* **20**, 2575–2585.

Vanderplaats, G N (1984), *Numerical optimization techniques for engineering design: With applications*, McGraw-Hill, New York.